# Electronic Raman scattering on the underdoped $HgBa_2Ca_2Cu_3O_{8+\delta}$ high-$T_c$ superconductor: The symmetry of the order parameter

A. Sacuto, J. Cayssol, and P. Monod
*Laboratoire de Physique de la Matière Condensée, Ecole Normale Supérieure, 24 rue Lhomond, F-75231 Paris Cedex 05, France*

D. Colson
*Physique de l'Etat Condensé, DRECAM/SPEC, CEA Saclay, F-91191, Gif-sur-Yvette, France*

(Received 17 September 1999)

In order to obtain high quality, reliable electronic Raman spectra of a high-$T_c$ superconductor compound, comparable with existing models, we have studied strongly underdoped $HgBa_2Ca_2Cu_3O_{8+\delta}$ with well prepared surface conditions. This choice was made such as to (i) minimize the overstoichiometry of oxygen $\delta$, (ii) avoid the need of phonon background subtraction from the raw data, and (iii) eliminate traces of parasitic phases identified and monitored on the crystal surface. Under these experimental conditions we are able to present the pure electronic Raman response function in the $B_{2g}$, $B_{1g}$, $A_{1g}+B_{2g}$, and $A_{1g}+B_{1g}$ channels. The $B_{2g}$ spectrum exhibits a linear frequency dependence (exponent $n=1.12\pm0.03$) at low energy whereas the $B_{1g}$ one shows a cubiclike dependence ($n=3.02\pm0.1$). The $B_{2g}$ and $B_{1g}$ spectra display a single well defined maximum at $5.6k_BT_c$ and $9k_BT_c$, respectively. In mixed $A_{1g}$ channels an intense electronic peak centered around $6.4k_BT_c$ is observed. The low-energy parts of the spectra (below 350 $cm^{-1}$) correspond to the electronic response expected for a pure $d_{x^2-y^2}$ gap symmetry (and can be fitted up to the gap energy for the $B_{1g}$ channel). However, in the upper parts (above 350 $cm^{-1}$), the relative position of the $B_{1g}$ and $B_{2g}$ peaks needs expanding the $B_{2g}$ Raman vertex to second-order Fermi surface harmonics to fit the data with the $d_{x^2-y^2}$ model. The sharper and more intense $A_{1g}$ peak appears to challenge the Coulomb screening efficiency present for this channel. As compared to previous data on more optimally doped, less stoichiometric Hg-1223 compounds, this work reconciles the electronic Raman spectra of underdoped Hg-1223 crystals with the $d_{x^2-y^2}$ model, provided that the oxygen doping $\delta$ is not too strong. This surprisingly strong sensitivity of the electronic Raman spectra to the low lying excitations induced by oxygen doping in the superconducting state is emphasized here and remains an open question.

## I. INTRODUCTION

Most of the recent investigations of inelastic light scattering by carriers (electronic Raman scattering) on high-$T_c$ superconductors are focused on the low-energy electronic spectra (up to the gap energy) obtained for different polarizations of the incident and scattered light. These experiments are carried out in order to study the angular dependence of the superconducting order parameter. Indeed, theoretical calculations initiated by Devereaux *et al.*[1] predicted specific power laws of the electronic Raman intensity at low energy depending on the superconducting gap symmetry and the light polarization. More precisely, for a $d_{x^2-y^2}$ gap (or a $|d_{x^2-y^2}|$ gap since Raman scattering is not phase sensitive), the $A_{1g}$ and $B_{2g}$ symmetries involved (deduced respectively from parallel and crossed polarizations along Cu-O direction) should display a linear frequency dependence whereas the $B_{1g}$ symmetry (obtained from crossed polarizations at 45° from the Cu-O direction) should exhibit a cubic frequency dependence below the gap energy.

In order to carry out with reasonable confidence such an investigation a number of experimental problems must be overcome. The main reason for the occurence of these difficulties stems out of the intrinsic weakness of the electronic Raman intensity which tends to be easily hindered by other contributions: intrinsic or extrinsic. These originate from (i) phonon scattering, (ii) parasitic phases (luminescence or Raman), and (iii) the effect of the overstoichiometry of the oxygen doping $\delta$.

The aim of this paper is to present pure electronic Raman measurements on high-$T_c$ superconductors. This implies to find the appropriate high-$T_c$ superconductors which allow us to eliminate or control the extra scattering contribution mentioned just above. We briefly discuss below each of these contributions together with their possible cure.

The first major experimental difficulty is that in most compounds, e.g., $La_{2-x}Sr_xCuO_4$, $YBa_2Cu_3O_{7-\delta}$ (Y-123), $Bi_2Sr_2CaCu_2O_{8+\delta}$ (Bi-2212) and $Tl_2Ba_2CuO_{6+\delta}$ (Tl-2201), an intense phonon structure is observed together with the weaker continuum of the electronic excitations.[2–5] In order to study the pure electronic Raman response function the phonon peaks have to be subtracted from the spectra. Vibrational structures are experimentally defined from the *N* state spectra and subtracted from the *S* state one. This procedure does not take into account the phonon temperature dependence (changes on the line shape and intensity). The intrinsic weakness of the electronic Raman scattering, resulting in a moderate signal to noise ratio, makes this procedure awkward. Despite these difficulties, qualitative agreement has been found with the $d_{x^2-y^2}$ model[2–5] although the exponent for the power law of the $B_{1g}$ channel is often dependent on the phonon subtraction protocole. Raw data (before subtrac-

 

tion of phonons) frequently exhibit an ambiguous exponent of the power law of the $B_{1g}$ channel. An attempt to avoid this problem[6] consisted in working on Tl-2201 superconductor, with the red excitation line such as to supress the resonance enhancement of the phonon scattering. Qualitative agreement with the $d_{x^2-y^2}$ model for the stoichiometric compound was obtained from raw data (without subtraction of phonon) in $B_{1g}$ channel.[6]

In our previous work, in contrast with the above mentioned compounds, we observed that the $HgBa_2Ca_2Cu_3O_{8+\delta}$ compounds exhibit much lower intensity phonon lines (about one order of magnitude) for polarization lying into the $CuO_2$ planes.[7,8] The decrease of the Raman activity of the $B_{1g}$ phonon can be understood by symmetry considerations with respect to the $CuO_2$ layer. Indeed it has been shown[9] that the $B_{1g}$ Raman phonon activity increases with the crystal electric field induced by the cationic planes above and below the $CuO_2$ plane. In the Hg-1223 mecurate the charge equivalence of the two cations ($Ba^{2+}$ and $Ca^{2+}$) minimizes the local electric field and thus reduces the Raman phonon activity. Conversely in the Y-123 compound where two differently charged cations ($Y^{3+}$,$Ba^{2+}$) are present above and below the $CuO_2$ plane, the Raman phonon activity is enhanced.

This favorable situation allowed us to carry out analysis of the Raman electronic spectra in the normal and superconducting states without dealing with the delicate handling of ''phonon subtraction.'' Another advantage to work with mercurates is that these compounds belong to the highest $T_c$ cuprate family which provides a larger spectral range below the superconducting gap frequency where the low-energy electronic spectrum can be analyzed.

The second major difficulty is due to the presence of parasitic phases on the surface of mercurate crystals. We have measured several Hg-1223 single crystals from various batches corresponding to different oxygen doping. Significant intrinsic variation of the shape of the low-energy spectrum (and thus changes of the power law) have been observed. These changes occur not only from batch to batch but, surprisingly, may also depend on the impact point of the laser beam onto the surface of the same crystal.[10] As will be shown below, electronic microscopy analyses revealed traces of $BaCuO_2$,$BaO_2$, and HgO which appear on as grown single crystal surfaces after exposure to air (for a few days). We discovered by a specific study on each of these phases (in bulk form) that their background is able to modify significantly the spectra even for minute quantities.

Finally the effect of the oxygen doping $\delta$ has to be taken into account. All studies carried out on underdoped, optimally doped, and overdoped high-$T_c$ superconductors revealed that the low-energy electronic spectra are very sensitive to the oxygen doping.[6,11–13] In contrast with the stoichiometric Tl-2201 compound, optimal doping of the Hg-1223 compound is reached for overstoichiometry of oxygen. However, excess oxygen introduces disorder into the Hg plane. Qualitatively, this oxygen overstoichiometry is observed to alter the electronic Raman spectrum at low energy, namely, introducing a linearlike frequency dependence visible in the $B_{1g}$ channel. In particular, our previous work[14] on electronic Raman spectra on overstoichiometric Hg-1223 crystals displayed a frequency dependence of the $B_{1g}$ channel in clear contradiction with the $d_{x^2-y^2}$ symmetry.

As a consequence, in order to avoid the phonon problem, to eliminate traces of parasitic phases and reduce the effect of the $\delta$ overstoichiometry, we have chosen to study strongly underdoped (UD) Hg-1223 crystals (nearly stoichiometric), cleaning the surface just before Raman measurements. Similar polishing has been shown to be compatible with high quality Y-123 crystals.[15]

Using these experimental conditions, we report pure electronic Raman spectra in the $N$ and $S$ states of the strongly UD Hg-1223 single crystals. Our main results are summarized as follows: in the $S$ state, the $B_{2g}$ electronic spectrum exhibits a linear frequency dependence at low-energy up to 350 $cm^{-1}$ whereas the $B_{1g}$ one shows a cubic frequency dependence up to 700 $cm^{-1}$.[16] The Raman spectra of the Hg-1223 in the $B_{2g}$ and $B_{1g}$ channels show well defined maxima at $5.6k_BT_c$ and $9k_BT_c$, respectively. Mixed $A_{1g}+B_{2g}$ and $A_{1g}+B_{1g}$ symmetries exhibit a strong maximum close to $6.4k_BT_c$.

Below 300 $cm^{-1}$ the electronic spectra of the strongly UD Hg-1223 for all the channels (and up to the gap energy for the $B_{1g}$) exhibit the electronic scattering expected for a pure $d_{x^2-y^2}$ gap. The quality of the experimental data offers strong evidence for the $d$ wave model. However, to reconcile the $B_{1g}$ and $B_{2g}$ peak positions, the $B_{2g}$ Raman vertices have to be expanded to the next higher-order of Fermi surface harmonics.[17] The strong maximum in mixed $A_{1g}+B_{2g}$ and $A_{1g}+B_{1g}$ channels cannot be simply explained by Coulomb screening. These last two points raise new questions about significance (within the $d_{x^2-y^2}$ framework) of the electronic maxima detected on the Raman spectra and the effective Coulomb screening of the $A_{1g}$ channel.

## II. CRYSTAL AND SURFACE CHARACTERIZATION

The crystallographic structure of Hg-1223 is tetragonal and belongs to the $^1D_{4h}$ space group[18] which allows us a direct comparison with theoretical calculations based on tetragonal symmetries. $HgBa_2Ca_2Cu_3O_{8+\delta}$ single crystals were grown by a single step synthesis as previously described[19,20] resulting in a strongly underdoped system with only a few stacking defects. Oxygen doping (when needed) was achieved by a separate oxygen annealing yielding a slightly underdoped system. The samples are parallelepipeds with typical $0.7\times0.7$ $mm^2$ square cross section and thickness 0.3 mm.

The [100] crystallographic direction lies at 45° of the edge of the square and the [001] direction is normal to the surface. This geometry helps us to align the crystallographic directions with respect to the light polarization.[21] dc magnetization measurements on strongly and slightly UD Hg-1223 crystals under field cooling (FC) and zero field cooling (ZFC) are displayed in Fig. 1. A sharp transition occurs at $T_c\sim121$ K, ($\Delta T_c\sim5$ K) for the stongly UD mercurate whereas the slightly UD Hg-1223 exhibits a larger transition width ($\Delta T_c\sim10$ K) with onset of diamagnetism around 133 K and a main transition close to 126 K. This most likely manifests a variation of the oxygen content inside the slightly UD crystals. We estimate the oxygen doping from the $T_c$-$\delta$ diagram recently established.[22] We find $\delta=0.12$ for $T_c=121$ K whereas $T_c=126$ K corresponds to $\delta=0.16$.[23] Up to now, the smallest value of $\delta$ experimentally obtained

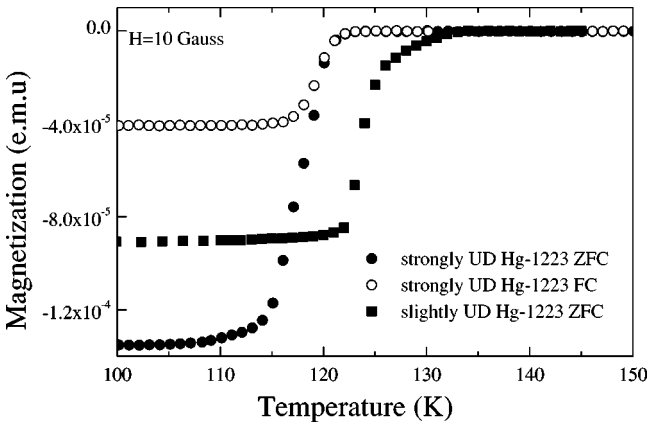


FIG. 1. dc magnetization in FC and ZFC of strongly and slightly UD Hg-1223 single crystals. The curve of the slightly UD Hg-1223 is taken from Ref. 14.

is close to 0.1.[22,24] Optimal doping is reached for $\delta=0.19$. Since over stoichiometry ($\delta$) refers to an excess of oxygen atoms randomly arranged within the Hg planes, optimal doping implies oxygen disorder in the Hg plane. In order to reduce the oxygen disorder inside the Hg-1223 structure it is therefore more appropriate to study UD Hg-1223 crystals. Moreover the UD Hg-1223 system is closer to a fourfold symmetry than an optimally doped one and is thus more appropriate to symmetry considerations. Resistivity values at $T_c$ is typically $\varrho(T_c)\sim(30-60)\ \mu\Omega$ cm (Ref. 25) showing the presence of very little (if any) impurities or defects. Particular attention has been paid to the surface quality. The mirrorlike surface of the freshly grown single crystal observed with an optical microscope reveals 0.1 $mm^2$ defect-free domains. However, after a few days of exposure to atmosphere new phases appear due to local decomposition. These new phases, undetectable by x-ray diffraction measurements, cluster together (10 $\mu$m) and are identified as $BaCuO_2$, $BaO_2$, HgO, and $Ca_{0.8}CuO_2$ by a local electron probe analysis. In order to eliminate these phases, we have polished the UD Hg-1223 single crystal surface just before Raman measurements. The single crystal is fixed by beeswax and polished by hand using 0.1 $\mu$m diamond paste and the adequate felt polishing disc. The crystal is then cleaned with acetone for spectroscopy (containing less than 0.1% of $H_2O$). We thus regenerate the original high quality defect-free surface of the crystal without local decomposition. Sometimes one or two inclusions of $Ca_{0.8}CuO_2$ (40 $\mu$m) are observed in the bulk and disapear upon further polishing. Scanning tunneling measurements on the polished surface reveal that the polishing streaks are less than 0.01 $\mu$m deep. An important optical test is that polished crystal surface under crossed polarization remains dark. This shows that the mechanical polishing does not alter the polarization of the reflected light.

## III. EXPERIMENTAL PROCEDURE

Raman measurements were performed with a double monochromator (U-1000 Jobin-Yvon) using single channel detection (EMI 9863B photomultiplier) and the $Ar^+$ laser 514.52 nm line. The spectral resolution was set at 2 $cm^{-1}$. The crystals immediately after polishing were mounted (in vacuum) on the cold finger of a liquid helium flow cryostat. The temperature was controlled by a CLTS resistance located on the backside of the cold finger. The incident laser spot is less than 100 $\mu$m in diameter and the intensity onto the crystal surface was kept below 25 W $cm^{-2}$ in order to avoid heating of the crystal. The incidence angle was 60°. The polarization is denoted in the usual way: $x$ [100] ($a$ axis), $y$ [010], $x'$ [110], $y'[1\bar{1}0]$. In order to compare our experimental data with the theoretical calculations,[1] the pure $B_{2g}$ $(xy)$ and $B_{1g}$ $(x'y')$ symmetries are needed. This requires that the incident electric field lies within the $xy$ plane. The incoming light being not normal to the surface, the crystal mount was rotated by 45° between the $B_{1g}$ and $B_{2g}$ spectra. The $A_{1g}+B_{1g}$ and $A_{1g}+B_{2g}$ symmetries are obtained from the $(xx)$ and $(x'x')$ polarizations, respectively. In order to probe the same area for all symmetries, the impact of the laser beam onto the crystal surface was precisely located before turning the crystal. Only large homogeneous surfaces have been selected. The least diffusive spot was selected in order to minimize the amount of spurious elastic scattering. Each Raman spectrum has been obtained after a sum of 40 scans. Each scan spanned between 25 and 1000 $cm^{-1}$ with an increment of 2 $cm^{-1}$ and an integration time of 3 s.

## IV. EXPERIMENTAL RESULTS

In view of the presence of the extra phases, we have performed systematic investigations of the hitherto ill reported Raman spectra of the parasitic phases related to mercury compounds, i.e., $BaO_2$, $BaCuO_2$, $Ba_2CuO_3$, HgO, $HgBaO_2$, $CaCO_3$. Measurements were carried out in the bulk form (powder) in the full range of interest (up to 1000 $cm^{-1}$) and in the same experimental conditions as those of the $B_{1g}$ and $B_{2g}$ spectra in the superconducting state (excitation line: 514.52 nm, light under crossed polarization, $T=13$ K). The results will be presented separatly[26] but can be summarized as follows: All these phases exhibit a nearly flat background together with characteristic phonon peaks[27] except the $BaO_2$ phase which shows a linear frequency dependent background extending up to 1000 $cm^{-1}$. This last phase can significantly alter the analysis of Raman spectra, as will be shown.

Imaginary parts of the Raman response function in the $S$ state and the $N$ state of the strongly UD Hg-1223 compound for the $B_{2g}$, $B_{1g}$, $A_{1g}+B_{2g}$, and $A_{1g}+B_{1g}$ channels are displayed in Fig. 2. The imaginary part of the susceptibilities in the superconducting and the normal states are obtained from Raman measurements at $T=13$ K and $T=295$ K, respectively. We present in Fig. 2 the most representative spectra of a serial of three sets of measurements perfomed on a strongly UD Hg-1223 crystal. In the following order, we have subtracted the dark current of the photomultiplier,[28] the Rayleigh scattering when present,[29] corrected the spectra for the response of the spectrometer and the detector and divided the spectra by the Bose-Einstein factor $n(\omega,T)+1=[1-\exp(\hbar\omega/k_BT)]^{-1}$. For the $B_{1g}$ and $B_{2g}$ channels obtained from crossed polarizations the response was scaled up by a factor 1.2 with respect to the $A_{1g}$ mixed channels in order to take into account the absorption of the half wave plate inserted between the analyzer and the entrance slit of the spectrometer. The insertion of the half wave plate allows us to

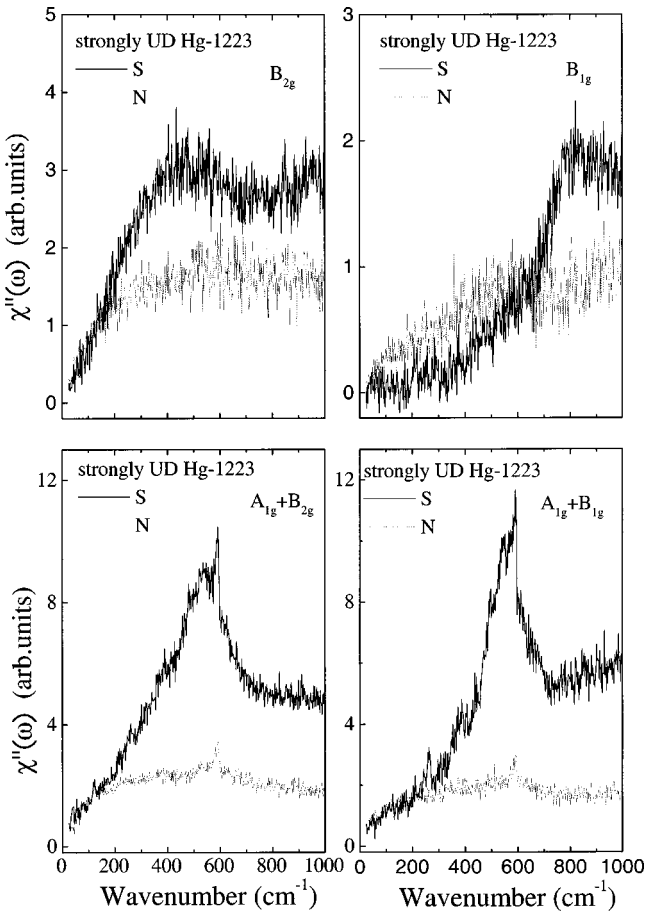


FIG. 2. Imaginary part of the electronic response function of the strongly UD Hg-1223 single crystal in the $B_{2g}$, $B_{1g}$, $A_{1g}+B_{2g}$, and $A_{1g}+B_{1g}$ channels. Solid and dashed lines correspond, respectively, to the superconducting and the normal state obtained from $T=13$ K and $T=295$ K. No phonon subtraction was necessary.

restore the same polarization inside the spectrometer for all the channels and thus benefit from the best configuration with respect to the grating factor efficiency.

In the *S* state, we clearly observe a linear frequency dependence at low energy (exponent $n=1.12\pm0.03$ from Fig. 2) with a well defined electronic maximum near 450 cm$^{-1}$ for the $B_{2g}$ channel whereas the $B_{1g}$ channel exibit no measurable electronic scattering below 200 cm$^{-1}$ in the limit of the photomultiplier detection and a nonlinear frequency dependence (exponent $n=3.02\pm0.1$ from Fig. 2) until we reach a maximum around 800 cm$^{-1}$.[16] We observe in Fig. 2, for both $B_{1g}$ and $B_{2g}$ channels, that the intensity of the electronic continuum above 800 cm$^{-1}$ in the *N* state is two times smaller than for the *S* state. This observation is puzzling since the optical absorption data give no reason to believe that there would be a superconductivity-induced change in the optical corrections to the Raman results that would reduce the high-$\omega$ *S*-state spectra in Fig. 2 to the level of the *N*-state spectra.[30]

In the $A_{1g}$ mixed symmetries, the electronic continuum shows a linear increase with respect to $\omega$ with a maximun centered around 550 cm$^{-1}$. The slope of the electronic scattering is twice larger in the $A_{1g}+B_{2g}$ spectrum than in the $A_{1g}+B_{1g}$ one. This can be attributed to the $B_{2g}$ linear contribution which increases the slope at low energy and broadens the low energy side of the $A_{1g}+B_{2g}$ maximum. As a consequence the $A_{1g}+B_{1g}$ peak is narrower than the $A_{1g}+B_{2g}$ one. A special remark can be made concerning the variation of the intensity of the phonon peaks at 540 and 590 cm$^{-1}$ in the *S* state in comparison with the *N* state. The intensities of these two phonon peaks are reduced by a factor of 3 when the temperature rises from $T=13$ to 150 K and decrease again by a factor of 1.2 between 150 and 295 K. The strong increase of the phonon intensity is clearly a superconductivity related effect since the phonons exhibit two regimes of intensity variations above and below $T_c$. The Raman phonon activities become similar to those obtained when electric fields are perpendicular to the *xy* plane, i.e., in *zz* polarization. The intensity enhancement of the phonons in the superconducting state has also been observed in other cuprates and a modified Raman scattering mechanism induced by a redistribution of the excited states in the superconducting state has been proposed.[31]

## V. COMPARISON WITH PREVIOUS WORK

In our previous work on slightly UD Hg-1223 mercurates, contrary to the present work on strongly UD Hg-1223, we reported a linear frequency dependence at low energy for the $B_{1g}$ spectrum (as well as for the $B_{2g}$) and one extra shoulder near 800 cm$^{-1}$ for the $A_{1g}$ spectrum in addition to the 550 cm$^{-1}$ peak.[14] These observations, in contradiction with the $d_{x^2-y^2}$ model, have been interpreted as the signature of an order parameter of lower symmetry. In view of the specific study on the parasitic phases mentioned above, we can now assign the presence of this shoulder to the presence of the $BaCuO_2$ phase. This is also supported by the observation on the $A_{1g}$ spectrum of the intense 640 cm$^{-1}$ phonon peak which is another signature of the $BaCuO_2$ phase. In the same way, we suspect that the multicomponents features observed by Zhou *et al.*[32] in the Raman spectra of Hg-1223 single crystals originate from vibrational modes of HgO and $BaCuO_2$ traces present on the crystal surface. Indeed the 340 and 640 cm$^{-1}$ peaks are characterisitc of HgO and $BaCuO_2$ spectra and correspond to the oxygen motions of the HgO and $BaCuO_2$ phases. Concerning the origin of the linear background previously reported in $B_{1g}$ spectrum at low energy[14] two scenarios can be considered: (i) light scattering from parasitic phases on the crystal surface, and (ii) light scattering induced by the oxygen overstoichiometry.[33]

Among different phases we quoted above, only the $BaO_2$ phase provides a frequency linear background and is able to compete even in minute quantities, with the superconducting signal.[26] Quantitative estimate[34] shows that less than 1% of $BaO_2$ is sufficient to produce scattering of the same order of magnitude as the electronic Raman coming from the *S* state. It is therefore necessary to thoroughly eliminate these phases before any optical investigation. However, two experimental observations show that this contribution is only partly relevant in our previous data: (i) an additionnal $BaO_2$ background which extends beyond to 1000 cm$^{-1}$ makes it difficult to interpret the decrease of the continuum above 800 cm$^{-1}$ observed on slightly UD mercurates; (ii) the temperature dependence of the electronic Raman intensity changes at $T_c$.[14] For these reasons we believe that the linear frequency dependence observed at low energy in the $B_{1g}$

channel mainly comes from the oxygen overstoichiometry doping rather than solely to the extrinsic $BaO_2$ phase. Many Raman experiments have been performed on high-$T_c$ superconductors as a function of the oxygen doping and reveal changes in the low energy electronic continuum.[6,11,12] Optimaly doped (stoichiometric) Tl-2201 compounds exhibit a cubiclike dependence in the $B_{1g}$ channel at low energy whereas the overdoped (overstoichiometric) Tl-2201 compounds show a linear dependence in the $B_{1g}$ channel at low energy.[6] An extreme case of the oxygen doping effect is present in underdoped Y-123 ($YBa_2Cu_3O_{6.5}$) in which case the $B_{1g}$ spectrum is temperature independent whereas the $B_{2g}$ spectrum exhibits a very strong pair-breaking peak.[13] Anisotropic impurity scattering is proposed to explain such a behavior.[13] In our previous data on slightly UD Hg-1223 crystal the linear background of $B_{1g}$ channel extends up to 600 $cm^{-1}$ consistent with an impurity scattering rate $\Gamma$ of the order of the gap $\Delta_0$ itself.[32] Such a high scattering rate should strongly reduce the critical temperature. This is in contradiction with $T_c=126$ K and resisitivity value $\rho(T_c)=(30-60)$ $\mu\Omega$ cm. We propose, without a specific model, that the linear background is induced by localized states generated by overstoichiometry of oxygen in the Hg-plane. This is supported by infrared reflectance measurements.[30] Indeed a strong damping at low energy ($T=15$ K) is observed in nearly optimally doped system as well as an intense and broad peak (near 184 $cm^{-1}$) on the real part of the optical conductivity. This peak is attributed to localized states. Conversely, in the strongly UD systems in which the oxygen doping is reduced with respect to the optimal one, there is no measurable residual damping at low frequency ($T=15$ K) and the 184 $cm^{-1}$ peak is narrower and weaker. This peak is often seen in high-$T_c$ superconductors and is very sensitive to the oxygen doping.[30,35–37]

## VI. MODEL FOR ELECTRONIC RAMAN SCATTERING

We compare our experimental data with the $d_{x^2-y^2}$ model. In the limit where the superconducting correlation length is much smaller than the optical penetration depth, the full complex response function for $T\rightarrow 0$ including the screening due to Coulomb interaction is given by[1,38,39]

$$\chi(\omega)=\chi_{\gamma\gamma}(\omega)-\frac{\chi_{\gamma 1}(\omega)\chi_{1\gamma}(\omega)}{\chi_{11}(\omega)}, \tag{1}$$

where the imaginary part of $\chi_{\gamma\delta}$ is defined by

$$\chi''_{\gamma\delta}(\omega)=\frac{2\pi N_F}{\omega}\mathrm{Re}\left\langle\frac{\gamma_{\mathbf{k}}\delta^{*}_{\mathbf{k}}\Delta^2_{\mathbf{k}}}{(\omega^2-4\Delta^2_{\mathbf{k}})^{1/2}}\right\rangle. \tag{2}$$

Here $\gamma_{\mathbf{k}}$ and $\delta_{\mathbf{k}}$ are general Raman vertices already described.[14] $N_F$ is the density of states for both spin orientations at the Fermi level, and the brackets indicate an average over the Fermi surface. $\Delta_{\mathbf{k}}$ stands for the superconducting, $\mathbf{k}$-dependent gap. Equation (2) vanishes in the limit of large frequency where we should recover the electronic scattering of the normal state. Therefore the normal state scattering contribution is not taken into account in the Raman response function derived in this work.

In the $d_{x^2-y^2}$ model, as computed by Devereaux *et al.*,[1,2] we approximate the Fermi surface as being a cylinder and take $\Delta_{\mathbf{k}}=\Delta_0\cos 2\theta$ for the gap and for the vertices: $\gamma_k^{B_{1g}}=\gamma_{B_{1g}}\cos 2\theta$, $\gamma_k^{B_{2g}}=\gamma_{B_{2g}}\sin 2\theta$, $\gamma_k^{A_{1g}}=\gamma_0+\gamma_{A_{1g}}\cos 4\theta$.

In $B_{1g}$ and $B_{2g}$ symmetries, $\chi_{\gamma 1}$ vanishes which implies that the last term in Eq. (1) drops out. In other words, the $B_{1g}$ and $B_{2g}$ symmetry are not screened. This is not the case for the $A_{1g}$ symmetry, and screening has to be properly taken into account. Nevertheless one sees easily from this equation that any $\mathbf{k}$-independent contribution to the Raman vertex drops out of the result.

In a pure $d_{x^2-y^2}$ model, the $B_{1g}$ channel is not sensitive to the nodes because the Raman vertex $\gamma_{\mathbf{k}}$ is zero by symmetry for $k_x=\pm k_y$. In contrast, the $k_x=0$ and $k_y=0$ regions do contribute, giving weight to the gap $\Delta_0$ in these directions. As a consequence the $B_{1g}$ spectrum displays a weak scattering at low energy and the calculated spectrum shows a $\omega^3$ frequency dependence with a maximum at $2\Delta_0$. Conversely, in the $B_{2g}$ channel, the Raman vertex $\gamma_{\mathbf{k}}$ is zero by symmetry for $k_x=0$ or $k_y=0$ and nonzero elsewhere, and hence provides weight in the $k_x=\pm k_y$ directions where the nodes are present. The $B_{2g}$ spectrum exhibits a linear low frequency dependence and a smeared gap. Finally the $A_{1g}$ channel is sensitive to both nodes and gap because the Raman vertex $\gamma_{\mathbf{k}}$ does not vanish in the $k_x=\pm k_y$, $k_x=0$, and $k_y=0$ regions. The $A_{1g}$ channel have to show a linear low $\omega$ behavior. This remains valid when we take into account the screening.

To provide a more realistic account of experimental results with respect to the theory we have included lifetime effects. We have chosen to include electronic damping by convoluting the bare spectra with a Lorentzian function. Depending on the electronic correlation model, the reduced half width of the Lorentzian can be taken as a constant ($\Gamma/2\Delta_0=a_0$), proportional to $\omega[\Gamma/2\Delta_0=a_1(\omega/2\Delta_0)]$ or proportional to $\omega^2[\Gamma/2\Delta_0=a_2(\omega/2\Delta_0)^2]$.

The $B_{1g}$ experimental spectrum exhibits a nearly cubic frequency dependence up to 700 $cm^{-1}$. Such a behavior imposes, whatever the type of damping, to use small values for the $a_0,a_1,a_2$ parameters. For $a_0=a_1=a_2=0.06$, we obtain satisfactory fits for the $B_{1g}$ spectrum, conversely if we increase by a factor 2 the reduced parameters, fits are in disagrement with experiments. As already explained[14] we have chosen to display fits for $\Gamma(\omega)=a_1\omega$. The calculated curves of the $B_{1g}$ and $B_{2g}$ spectra for three values of the $a_1$ parameter are shown in Fig. 3. The half width at half maximum of the $B_{1g}$ peak is seen to double as the $a_1$ parameter is increased by a factor 5. This dependence reduces the choice of the $a_1$ parameter to values close to 0.06 in order to be in agreement with the experimental data. This value of the damping parameter $a_1$ should be compared with the value of 0.15 previously obtained on more oxygen disordered Hg-1223.[14] The fact that in this latter case $T_c$ is increased may appear paradoxical. We are forced to conclude, in that case, that the effect of doping overwhelms the effect of scattering by disorder. A similar conclusion can be reached from infrared measurements.[30]

The theoretical spectra in $B_{1g}$, $B_{2g}$, and $A_{1g}$ screened channels for $a_1=0.06$ are displayed in Fig. 4. Fits have been calculated from the strongly UD Hg-1223 data. The $2\Delta_0$ gap has been defined from the $B_{1g}$ spectrum since the $B_{1g}$ vertex

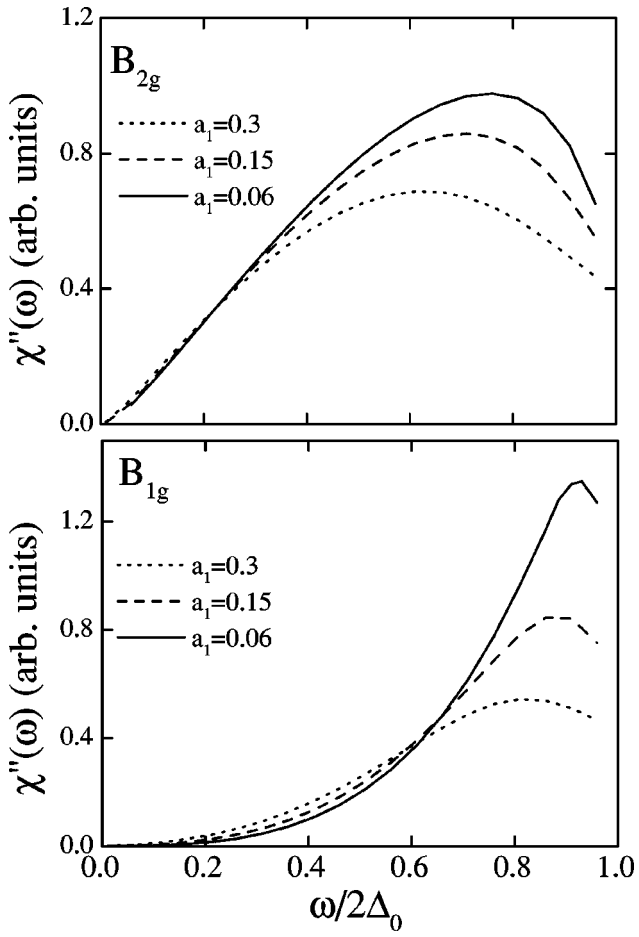


FIG. 3. Theoretical curves of the $B_{1g}$ and $B_{2g}$ spectra for different values of the $a_1$ damping parameter ($\Gamma = a_1\omega$).

probes directly the $\Delta_0$ amplitude. We have chosen to adjust the lower part of the calculated curves to the experimental data. Below 300 $cm^{-1}$ we find a very good agreement between theoretical and experimental data for all three channels and up to the gap for the $B_{1g}$ channel. However the fits are not satisfactory at higher energy (above 300 $cm^{-1}$) for the $B_{2g}$ and $A_{1g}$ channels. First the $B_{2g}$ maximum of the calculated spectrum (700 $cm^{-1}$) is clearly far away from the $B_{2g}$ experimental one (450 $cm^{-1}$) as it is seen in Fig. 4. As a consequence the calculated frequency ratio between the $B_{1g}$ and $B_{2g}$ peaks positions (1.2) does not correspond to the experimental one (1.6) obtained from the Hg-1223 spectra. Secondly the calculated curve of the $A_{1g}$ screened spectrum is a broad peak centered around 700 $cm^{-1}$ whereas we get experimentally a sharper (width at half maximum: 200 $cm^{-1}$) and more intense peak near 550 $cm^{-1}$.

Concerning the first point ($B_{2g}$ spectrum) we propose to expand the $B_{2g}$ vertex to higher order as was already done for the $A_{1g}$ vertex. The justification of this procedure is based on the fact that the Fermi surface is anisotropic. The $B_{2g}$ vertex is expected to be more sensitive to additional harmonic terms than the $B_{1g}$ vertex because the $B_{2g}$ vertex probes a region where the gap changes drastically (nodes of the gap). It is then possible to reconcile experiments to the $d_{x^2-y^2}$ model by expanding the $B_{2g}$ vertex to the next order of the Fermi surface harmonics.[1] Indeed including higher order Fermi surface harmonics in the Raman vertices

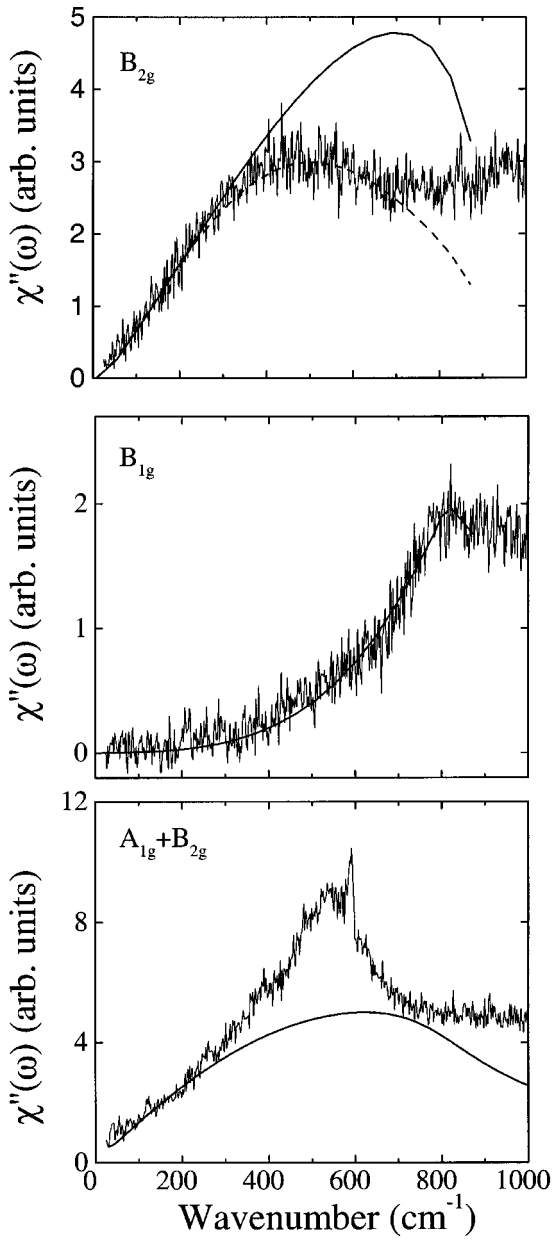


FIG. 4. Comparison between the experimental data and the $d_{x^2-y^2}$ model. The calculated curves obtained from the $B_{1g}$, $B_{2g}$, and $A_{1g}$ vertices defined in Eq. (3) are shown in solid lines. The dashed line corresponds to the $B_{2g}$ calculated curve including the second order expansion of the $B_{2g}$ vertex ($\beta = 0.4$). For all the calculations $a_1 = 0.06$.

changes the relative positions of the $B_{1g}$ and $B_{2g}$ peaks. Cardona *et al.*[40] showed that the $B_{1g}$ peak shifts down when varying the $\alpha$ parameter related to the contribution of the second Fermi surface harmonics $\gamma_{B_{1g}}[\cos 2\theta - \alpha \cos 6\theta]$. By taking $\gamma_k^{B_{2g}} = \gamma_{B_{2g}}[\sin 2\theta - \beta \sin 6\theta]$, we find that the $B_{2g}$ peak softens as $\beta$ increases (see Fig. 5). As expected this softening is even larger when we consider the $B_{2g}$ vertex than for the $B_{1g}$ vertex. The calculated curve of the $B_{2g}$ spectrum obtained for $\beta = 0.4$ is displayed on Fig. 4. We find an agreement between our calculated and experimental curves up to 700 $cm^{-1}$. These results are consistent with the $d_{x^2-y^2}$ model, considering the deviation away from the cylindricity of the Fermi surface when calculating the vertices. The rela-

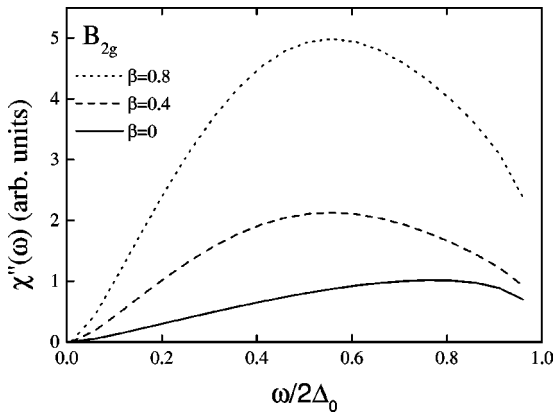


FIG. 5. Theoretical curves of the $B_{2g}$ response for $\beta=0$, 0.4, 0.8 ($a_1=0.06$).

tive deviation of the Raman vertex is assumed for simplicity to be larger than that of the wave vector on the Fermi surface. Best fits could be further improved by taking into account electronic scattering in the normal state, but this is not done here.

Concerning the second point ($A_{1g}$ spectrum) the Coulomb screening present in the Raman scattering process might be not as efficient as has been supposed. Strong mass fluctuations induced by interlayer coupling or several sheets of $CuO_2$ planes as proposed elsewhere,[40] could decrease the $A_{1g}$ scattering efficiency. On the other hand expansion to higher order of the $A_{1g}$ vertex has to be explored.

## VII. CONCLUSION

In conclusion we have especially investigated strongly underdoped $HgBa_2Ca_2Cu_3O_{8+\delta}$ single crystals in order to reduce the oxygen disorder in the Hg-plane taking care to eliminate parasitic phases on the crystal surface. Under these improved experimental conditions we are able to report with good accuracy the pure electronic Raman scattering (without subtraction of phonons) in the $B_{2g}$,$B_{1g}$,$A_{1g}+B_{2g}$, and $A_{1g}+B_{1g}$ channels. The $d_{x^2-y^2}$ model fits quite well with the low energy part (below 350 $cm^{-1}$) of the spectra for the $B_{2g}$ and $A_{1g}$ symmetries and up to the gap energy for $B_{1g}$. However, in order to reconcile the upper part of the $B_{1g}$ and $B_{2g}$ spectra (above 350 $cm^{-1}$) with the $d_{x^2-y^2}$ model, we have to expand the $B_{2g}$ vertex to the next order of Fermi surface harmonics. The sharp and intense electronic maximum in mixed $A_{1g}$ symmetries remains difficult to interpret in the framework of the $d_{x^2-y^2}$ model. This last point raises new questions about the $A_{1g}$ screening efficiency. Experimentally, this work on near stoichiometric Hg-1223 compounds as compared to previous work on less stoichiometric compounds highlights the importance of the oxygen overstoichiometry on the low energy excitations as revealed by the frequency dependence, cubic or linear of the $B_{1g}$ electronic Raman spectra. This surprisingly strong effect already reported in a number of high-$T_c$ cuprates is understood in only a qualitative way and bears directly on the dynamics of the low lying electronic states in the superconducting state.

## ACKNOWLEDGMENTS

We thank T. Timusk, J. J. McGuire, R. Combescot, N. Bontemps, N. Sandler, M. T. Béal-Monod, R. Hackl, B. Jusserand, E. Ya. Sherman, P. Calvani, and R. Lobo for very fruitful discussions. We are grateful to M. Jouanne and J. F. Morhange for their collaboration with the Raman spectrometer (LMDH, Paris VI). We also wish to acknowledge S. Poissonnet and L. Schmirgeld-Mignot for the chemical analysis by electron probe.

[1] T.P. Devereaux, D. Einzel, B. Stadlober, R. Hackl, D.H. Leach, and J.J. Neumeier, Phys. Rev. Lett. **72**, 396 (1994); T.P. Devereaux and D. Einzel, Phys. Rev. B **51**, 16 336 (1995); **54**, 15 547 (1996).

[2] X.K. Chen, J.C. Irwin, H.J. Trodhal, T. Kimura, and K. Kishio, Phys. Rev. Lett. **73**, 3290 (1994).

[3] N. Nemetschek, R. Hackl, M. Opel, R. Philipp, M.T. Béal-Monod, J.B. Bieri, K. Maki, A. Erb, and E. Walker, Eur. Phys. J. B **5**, 495 (1998).

[4] T. Staufer, R. Nemetschek, R. Hackl, P. Müller, and H. Veith, Phys. Rev. Lett. **68**, 1069 (1992).

[5] L.V. Gasparov, P. Lemmens, M. Brinkmann, N.N. Kolesnikov, and G. Güntherodt, Phys. Rev. B **55**, 1223 (1997).

[6] Moonsoo Kang, G. Blumberg, M.V. Klein, and N.N. Kolesnikov, Phys. Rev. Lett. **77**, 4434 (1996).

[7] A. Sacuto, A. Lebon, D. Colson, A. Bertinotti, J.-F. Marucco, and V. Viallet, Physica C **259**, 209 (1996); Similar observations have been made by X. Zhou, M. Cardona, D. Colson, and V. Viallet, Phys. Rev. B **55**, 12 770 (1997).

[8] A. Sacuto, R. Combescot, N. Bontemps, P. Monod, V. Viallet, and D. Colson, Europhys. Lett. **39**, 207 (1997).

[9] E.I. Rashba and E.Ya. Sherman, Pis'ma Zh. Éksp. Teor. Fiz. **47**, 404 (1988) [JETP Lett. **47**, 482 (1988)]; E.Ya. Sherman, R. Li, and R. Feile, Phys. Rev. B **52**, R15 757 (1995).

[10] This last observation was made by inserting a video camera just behind the entrance slit of the spectrometer which allowed us to precisely choose (50 $\mu$m) the laser spot on the crystal surface. Clean domains where data are consistent with each other have been carefully selected in our previous work (Ref. 14).

[11] L.V. Gasparov, P. Lemmens, N.N. Kolesnikov, and G. Güntherodt, Phys. Rev. B **58**, 11 753 (1998).

[12] X.K. Chen, J.G. Naeini, K.C. Hewitt, J.C. Irwin, R. Liang, and W.N. Hardy, Phys. Rev. B **56**, R513 (1997).

[13] M. Opel, R. Nemetschek, C. Hoffmann, P.F. Müller, R. Philipp, R. Hackl, H. Berger, L. Forro, A. Erb, and E. Walker, J. Phys. Chem. Solids **59**, 1942 (1998); M. Opel, R. Nemetschek, C. Hoffmann, R. Philipp, P.F. Müller, R. Hackl, I. Tüttö, H. Berger, A. Erb, B. Revaz, E. Walker, H. Berger, and L. Forro, cond-mat/9908272 (unpublished).

[14] A. Sacuto, R. Combescot, N. Bontemps, C.A. Müller, V. Viallet, and D. Colson, Phys. Rev. B **58**, 11 721 (1998).

[15] C.P. Bidinosti, W.N. Hardy, D.A. Bonn, and R. Liang, Phys. Rev. Lett. **83**, 3277 (1999).

[16] Preliminary results on strongly UD Hg-1201 mercurates ($T_c$

~55 K) exhibit the same behavior as the strongly UD Hg-1223 one at low energy, i.e., linear and cubic dependence for $B_{2g}$ and $B_{1g}$, respectively.

[17] P.B. Allen, Phys. Rev. B **13**, 1416 (1976).

[18] M. Cantoni, A. Schilling, H.-U. Nisen, and H.R. Ott, Physica C **215**, 11 (1993).

[19] D. Colson, A. Bertinotti, J. Hammann, J.-F. Marucco, and A. Pinatel, Physica C **233**, 231 (1994); A. Bertinotti *et al. ibid.* **250**, 213 (1995).

[20] A. Bertinotti, D. Colson, J-F. Marucco, V. Viallet, J. Le Bras, L. Fruchter, C. Marcenat, A. Carrington, and J. Hammann, in *Studies of High Temperature Superconductors*, edited by Narlikar (Nova Science, New York, 1997).

[21] The uncertainty inherent to this procedure is believed to be negligeable.

[22] V. Viallet-Guillem, Ph.D. thesis, University of Paris Sud, 1998.

[23] In Ref. 14 we quoted $\delta$ less than 0.1 for $T_c = 126$ K. This value was later corrected by thermogravimetry measurements to $\delta = 0.16$. Hence the crystal used in this previous work belongs to the slightly UD system.

[24] A. Fukuoka, A. Tokiwa-Yamamoto, M. Iitoh, R. Usami, S. Adachi, and K. Tanabe, Phys. Rev. B **55**, 6612 (1997).

[25] A. Carrington, D. Colson, Y. Dumont, C. Ayache, A. Bertinotti, and J.F. Marucco, Physica C **234**, 1 (1994).

[26] A. Sacuto, D. Colson, J. Cayssol, B. Jusserand, and P. Monod, Physica C (to be published).

[27] The HgO phase exhibits two phonon peaks at 340 and 560 $cm^{-1}$. The $HgBaO_2$ spectrum shows three peaks at 200, 340, and 645 $cm^{-1}$. The $BaO_2$ spectrum shows a phonon structure close to 840 $cm^{-1}$. The $BaCuO_2$ spectrum exhibits two peaks at 590 and 640 $cm^{-1}$ and one shoulder near 800 $cm^{-1}$. The $Ba_2CuO_3$ spectrum presents an intense phonon peak at 560 $cm^{-1}$ and the $CaCO_3$ spectrum exhibits three peaks at 160, 289, and 712 $cm^{-1}$.

[28] The dark current is constant and its intensity corresponds approximatively to 30% of the $B_{2g}$ signal at 13 K and above 800 $cm^{-1}$.

[29] There is no correction for cross polarization ($B_{1g}$ and $B_{2g}$) and a small contribution is removed by extrapolation below 50 $cm^{-1}$ for parallel polarizations ($A_{1g}$).

[30] J. J. McGuire, M.Windt, T. Startseva, T. Timusk, D. Colson, and V. Viallet-Guillen (unpublished).

[31] O.V. Misochko, E.Ya. Sherman, N. Umesaki, K. Sakai, and S. Nakashima, Phys. Rev. B **59**, 11 495 (1999).

[32] X. Zhou, M. Cardona, D. Colson, and V. Viallet, Physica C **282-287**, 1007 (1997).

[33] We note that the effects of the oxygen overstoichiometry reported here do not preclude our initial interpretation in terms of a modified order parameter symmetry (Ref. 14).

[34] We have estimated the Raman intensity as a function of the $BaO_2$ phase percent. It was done from the Raman spectrum of the $BaO_2$ powder (in the bulk form) obtained in the same experimental conditions as the $B_{2g}$ and $B_{1g}$ spectra in the $S$ state. 100% of illuminated bulk of $BaO_2$ gives 500 arb. units at 300 $cm^{-1}$.

[35] T.P. Devereaux, Phys. Rev. Lett. **74**, 4313 (1995).

[36] D.N. Bazov, B. Dabrowski, and T. Timusk, Phys. Rev. Lett. **81**, 2132 (1998).

[37] S. Lupi, P. Maselli, M. Capizzi, and P. Calvani, Phys.Rev. Lett. **83**, 4852 (1999); R.P.S.M. Lobo, F. Gervais, and S.B. Oseroff, Europhys. Lett. **37**, 341 (1997).

[38] M.V. Klein and S.B. Dierker, Phys. Rev. B **29**, 4976 (1984).

[39] Equations (6) and (7) mentioned in Ref. 14 have to be replaced by Eqs. (1) and (2) cited here.

[40] M. Cardona, T. Strohm, and X. Zhou, Physica C **282-287**, 222 (1997); T. Strohm and M. Cardona, Phys. Rev. B **55**, 12 725 (1997).